EARTH SURFACE PROCESSES AND LANDFORMS, VOL 23, 159–169 (1998)

THE EFFECT OF ROUGHNESS CONFIGURATION ON VELOCITY PROFILES IN AN ARTIFICIAL CHANNEL

ELLEN E. WOHL[1*] AND HIROSHI IKEDA[2]

[1]*Department of Earth Resources, Colorado State University, Fort Collins, Colorado 80523, USA*
[2]*Environmental Research Center, University of Tsukuba, Tsukuba, Ibaraki 305, Japan*

Received 9 August 1996; Revised 21 March 1997; Accepted 21 May 1997

ABSTRACT

In order to determine the effect of bed roughness on velocity distribution, we used seven different configurations of bed roughness, with 16 test runs of varying discharge and slope for each configuration. For each run, one-dimensional velocity profiles were measured at 1 cm vertical increments over the crest of the roughness element, and at intervals of 4·25 cm downstream. Results indicate that velocity profile shape remains fairly constant for a given slope and roughness configuration as discharge increases. As slope increases, the profiles become less linear, with a much larger near-bed velocity gradient and a more pronounced velocity peak close to 0·6 flow depth at the measurement point immediately downstream from the roughness element. The zone of large near-bed velocity gradients increases in both length and depth as roughness concentration decreases, up to a length/height ratio of about 9, at which point maximum flow resistance occurs. Longitudinal roughness elements do not create nearly as much flow resistance as do transverse elements. Rates of velocity increase suggest that roughness elements spaced at a length/height ratio of about 9 are most effective at creating flow resistance over a range of discharges in channels with steeper slopes. © 1998 John Wiley & Sons, Ltd.

Earth surf. process. landforms, **23,** 159–169 (1998)
No. of figures: 6 No. of tables: 1 No. of refs: 13
KEY WORDS: bed roughness; velocity profile

INTRODUCTION

Irregularities along the bed of a channel have long been recognized to affect the velocity distribution of flow within the channel by increasing bed friction and creating flow separation and turbulent velocity fluctuations. Early experimental studies attempted to quantify these effects by experimentally measuring flow resistance along a flume during test runs with variously shaped roughness elements (Johnson and LeRoux, 1946; Morris, 1955; Rouse, 1965; Nowell and Church, 1979). Several subsequent investigators (e.g. Nowell and Church, 1979; Davies, 1980; Whittaker and Jaeggi, 1982; Hassan and Reid, 1990) examined the effect of bedform spacing on flow resistance in both natural and artificial channels. These studies established that: (i) the highest values of flow resistance are associated with intermediate densities of roughness elements because vortex generation and dissipation in the lee of one element is not complete before the flow meets the next element; (ii) a rise and fall in roughness length with increasing boundary roughness occurs in association with variously shaped and grouped roughness elements; and (iii) roughness element/bedform shape affects the spacing at which maximum flow resistance occurs. In addition, Robert *et al*. (1992) used flume experiments to demonstrate an increase in boundary shear stress and a change in velocity profile shape at a transition from close-packed roughness to a bed with more widely spaced obstacles.

Previous studies have mainly focused on the effect of bedform shape and spacing on flow resistance, generally for a single discharge or slope. Flow resistance has been judged by a single measure, such as resistance coefficient. In the research presented here, we used a simple experimental design to evaluate how velocity distribution and flow resistance vary across seven different roughness configurations at various values of channel slope and discharge. Thus, rather than evaluating flow resistance in terms of a single index at fixed

* Correspondence to: E. E. Wohl

CCC 0197-9337/98/020159–11 $17.50

Table I. Summary data for flume runs. Runs are numbered consecutively for each case (run 1 is 2 $l s^{-1}$ and 0·6 per cent slope; run 16 is 16 $l s^{-1}$ and 5 per cent slope). Mean flow depth is above the ribs

Discharge ($l s^{-1}$)	Slope (%)	Surface velocity ($cm s^{-1}$)	Mean velocity ($cm s^{-1}$) [std dev]	Mean flow depth (cm)	d/h*	λ_d†	v‡
Case 1. Transverse ribs spaced at 4·25 cm (1 rib width); e = 0·89, L/h=*2·24*							
2	0·6	48	33 [2]	2·3	0·60	0·0026	
4	0·6	68	55 [7]	3·5	0·92	0·0014	
8	0·6	87	75 [7]	5·5	1·45	0·0012	
16	0·6	104	98 [12]	9·2	2·42	0·0012	65
2	1·2	60	42 [6]	1·8	0·49	0·0025	
4	1·2	82	64 [5]	3·0	0·78	0·0018	
8	1·2	103	94 [11]	4·8	1·25	0·0013	
16	1·2	118	123 [19]	7·8	2·04	0·0013	81
2	2·5	72	52 [8]	1·6	0·42	0·0029	
4	2·5	96	78 [6]	2·5	0·66	0·0020	
8	2·5	122	114 [15]	4·0	1·07	0·0015	
16	2·5	138	146 [43]	6·8	1·80	0·0016	94
2	5·0	83	56 [0]	1·4	0·37	0·0044	
4	5·0	111	106 [11]	2·1	0·55	0·0018	
8	5·0	141	135 [12]	3·6	0·93	0·0019	
16	5·0	157	170 [16]	5·7	1·50	0·0019	114
Case 2. Transverse ribs spaced at 12·75 cm (3 rib widths); e = *0·22*, L/h = *4·47*							
2	0·6	51	33 [15]	4·0	1·07	0·0045	
4	0·6	56	38 [16]	4·6	1·22	0·0039	
8	0·6	63	51 [20]	7·8	2·04	0·0037	
16	0·6	90	73 [24]	11·2	2·93	0·0026	40
2	1·2	57	35 [17]	3·2	0·86	0·0064	
4	1·2	61	39 [17]	3·6	0·96	0·0058	
8	1·2	75	60 [22]	6·4	1·70	0·0044	
16	1·2	95	86 [31]	9·4	2·46	0·0031	51
2	2·5	59	39 [20]	3·0	0·80	0·0097	
4	2·5	72	45 [20]	3·6	0·95	0·0087	
8	2·5	87	73 [28]	5·2	1·37	0·0048	
16	2·5	122	109 [42]	8·0	2·10	0·0033	70
2	5·0	52	43 [19]	7·2	1·91	0·0382	
4	5·0	78	52 [21]	8·6	2·26	0·0312	
8	5·0	116	94 [40]	4·3	1·13	0·0048	
16	5·0	152	123 [48]	6·8	1·78	0·0044	100
Case 3. Transverse ribs spaced at 29·75 cm (7 rib widths); e = *0·11*, L/h = *8·95*							
2	0·6	23	18 [8]	2·8	0·75	0·0107	
4	0·6	38	32 [11]	5·2	1·38	0·0063	
8	0·6	48	41 [13]	8·7	2·29	0·0064	
16	0·6	62	60 [17]	14·1	3·71	0·0048	42
2	1·2	32	20 [10]	2·3	0·60	0·0141	
4	1·2	43	34 [14]	4·6	1·22	0·0098	
8	1·2	49	47 [15]	7·6	2·00	0·0084	
16	1·2	66	70 [22]	13·1	3·45	0·0066	50
2	2·5	41	25 [13]	1·9	0·50	0·0149	
4	2·5	53	38 [16]	3·7	0·97	0·0126	
8	2·5	64	54 [17]	6·0	1·59	0·0101	
16	2·5	92	82 [23]	12·6	3·33	0·0092	57
2	5·0	26	30 [18]	1·9	0·50	0·0207	
4	5·0	39	44 [15]	3·8	1·01	0·0192	
8	5·0	56	56 [21]	6·2	1·63	0·0194	
16	5·0	104	109 [40]	11·0	2·91	0·0091	79
Case 4. Transverse ribs spaced at 63·75 cm (15 rib widths); e = *0·06*, L/h = *17·90*							
2	0·6	27	22 [12]	2·5	0·65	0·0064	
4	0·6	38	35 [15]	4·4	1·15	0·0044	
8	0·6	46	49 [16]	7·6	2·00	0·0039	
16	0·6	68	70 [19]	11·8	3·11	0·0030	48
2	1·2	30	23 [17]	2·2	0·57	0·0102	
4	1·2	43	39 [17]	4·0	1·05	0·0064	
8	1·2	51	54 [15]	6·7	1·76	0·0056	
16	1·2	68	75 [20]	10·8	2·86	0·0047	52

(continued)

Table I. (continued)

Discharge ($l s^{-1}$)	Slope (%)	Surface velocity ($cm s^{-1}$)	Mean velocity ($cm s^{-1}$) [std dev]	Mean flow depth (cm)	d/h*	λ_d†	v‡
2	2·5	–	29 [23]	2·7	0·72	0·0157	
4	2·5	41	45 [25]	4·0	1·07	0·0097	
8	2·5	62	70 [25]	6·9	1·81	0·0069	
16	2·5	71	84 [27]	9·7	2·55	0·0067	55
2	5·0	43	61 [26]	3·8	0·99	0·0100	
4	5·0	62	91 [28]	4·7	1·23	0·0056	
8	5·0	82	115 [32]	7·0	1·85	0·0052	
16	5·0	100	128 [40]	10·1	2·67	0·0060	67
Case 5. Plane bed; e = *1·00*							
2	0·6	63	58 [0]	2·0			
4	0·6	77	61 [2]	3·4			
8	0·6	92	96 [10]	6·0			
16	0·6	105	119 [11]	9·1			
2	1·2	75	–	2·2			
4	1·2	91	100 [0]	4·0			
8	1·2	108	122 [7]	6·6			
16	1·2	129	146 [13]	10·8			
2	2·5	95	–	2·6			
4	2·5	118	110 [0]	4·0			
8	2·5	138	154 [4]	6·8			
16	2·5	160	184 [80]	12·8			
2	5·0	124	–	1·9			
4	5·0	147	144 [0]	3·9			
8	5·0	194	186 [2]	6·2			
16	5·0	198	200 [0]	10·7			
Case 6. Longitudinal ribs spaced at 8·5 cm (2 rib widths)							
2	0·6	68	68 [3]	5·4	1·42	0·0014	
4	0·6	86	77 [3]	6·5	1·71	0·0014	
8	0·6	100	86 [4]	8·0	2·09	0·0013	
16	0·6	104	112 [12]	11·2	2·95	0·0011	
2	1·2	87	78 [4]	4·8	1·26	0·0019	
4	1·2	105	91 [6]	5·6	1·47	0·0017	
8	1·2	112	114 [11]	7·2	1·88	0·0014	
16	1·2	135	138 [17]	9·8	2·57	0·0013	
2	2·5	99	104 [10]	4·0	1·07	0·0018	
4	2·5	110	125 [15]	5·0	1·30	0·0016	
8	2·5	129	141 [14]	6·2	1·64	0·0015	
16	2·5	152	167 [16]	8·1	2·13	0·0014	
2	5·0	132	144 [7]	3·0	0·79	0·0014	
4	5·0	141	158 [16]	4·2	1·10	0·0016	
8	5·0	180	185 [16]	5·3	1·40	0·0015	
16	5·0	213	200 [–]	6·0	1·58	0·0015	
Case 7. Longitudinal ribs spaced at 4·25 cm (1 rib width)							
2	0·6	65	58 [3]	5·6	1·47	0·0020	
4	0·6	78	69 [3]	6·6	1·74	0·0017	
8	0·6	93	79 [6]	8·6	2·26	0·0017	
16	0·6	110	103 [10]	11·8	3·12	0·0014	
2	1·2	74	70 [6]	5·0	1·33	0·0025	
4	1·2	96	85 [7]	5·8	1·54	0·0020	
8	1·2	111	105 [10]	7·3	1·92	0·0016	
16	1·2	130	131 [17]	9·5	2·50	0·0014	
2	2·5	88	96 [9]	4·4	1·14	0·0023	
4	2·5	110	116 [13]	5·0	1·30	0·0018	
8	2·5	133	136 [12]	6·4	1·68	0·0017	
16	2·5	154	171 [16]	8·4	2·20	0·0014	
2	5·0	118	138 [9]	3·6	0·93	0·0018	
4	5·0	148	160 [12]	4·3	1·31	0·0016	
8	5·0	175	186 [14]	5·4	1·41	0·0015	
16	5·0	222	200 [2]	6·8	1·78	0·0017	

* Ratio of average flow depth to rib height
† Resistance coefficient, λ_d (see Equation 1 in text)
‡ Difference in mean velocity (in $cm s^{-1}$) between 2 $l s^{-1}$ and 16 $l s^{-1}$ for a given slope and roughness configuration

slope and discharge, we focused on changes in velocity profiles and spatial velocity patterns, relative to changes in channel roughness, slope and discharge. Our objective in performing these experiments was to address the following questions: (1) For a given roughness configuration, how does the velocity distribution vary with discharge, and with slope? (2) For the roughness configurations tested here, which configurations maximize energy expenditure at all discharges? (3) What are the possible implications of the experimental results for energy expenditure and sediment transport along natural channels?

METHODS

The experimental runs reported here were conducted in a flume 21 cm wide, 18 cm deep, and 8 m long, at the Environmental Research Center of the University of Tsukuba. We conducted the runs under uniform, steady-flow conditions; the average energy, water-surface, and channel-bed gradients were equal along the length of the flume during each run. We used seven different roughness configurations, with 16 test runs for each configuration (Table I). Discharge was varied at 2, 4, 8 and 16 l s^{-1}, and slope was varied at 0·6, 1·2, 2·5 and 5 per cent increments. The ribs mentioned in Table I were rectangular blocks of wood 4·25 cm wide, that protruded 3·8 cm above the channel floor. The ribs thus form relatively short-crested roughness elements (length/height ratio of 1·12) and have flat crests. For the transverse configurations, these ribs spanned the entire channel width perpendicular to flow. We began in Case 1 with the ribs spaced one rib-width apart, and for successive cases we removed every alternative rib. Case 5 was a plane bed. For the two longitudinal configurations, the ribs ran for 4 m along the length of the flume parallel to flow direction. For Case 6, the ribs were placed at the base of the flume walls, and for Case 7 they were placed one rib-width apart. The bed between ribs was a plywood sheet with the same surface roughness as the surface of the ribs.

Flow depth for each run was measured using a point gauge attached to the top of the flume. Surface velocity was measured with paper floats and a stopwatch. One-dimensional velocity profiles were measured using a Kenek VM-201H two-dimensional electromagnetic current meter at a time constant of 0·5 (we ignored the second measurement dimension). This meter has a cylindrical head 1·5 cm long and 0·4 cm wide, with sensors at its centre. The head is oriented upright (long axis perpendicular to channel bed) in the flow, so that the minimum height above the bed at which velocity can be measured is 0·75 cm. Velocity profiles for each run were measured at the same points: for transverse configurations, one profile centred above a rib, and succeeding profiles centres one rib-width downstream, up to eight rib-widths for Cases 3 and 4; for longitudinal configurations, one profile centred above a rib, one centred over the space between the ribs, and one profile one-quarter of the distance between the ribs (Case 6). In both cases, measurements were taken 2 m downstream from the start of the ribs. Profiles were measured at 1 cm vertical intervals from the channel bed to the top of the water column, with only the mean value of the x-component of velocity being recorded.

Using the velocity profile data, velocity mean and standard deviation were calculated for each run (Table I). The number of measurements used to calculate velocity mean and standard deviation for each run varied from five measurements for Case 1, run 1, to 120 measurements for Case 4, run 4. Velcosity mean and standard deviation, along with surface velocity, were regressed against channel slope and discharge to evaluate correlations among the variables. We also plotted the velocity profiles and constructed isovel maps for the line of velocity measurements as a means of assessing spatial patterns of velocity. Resistance to flow produced by various roughness configurations was calculated from the resistance coefficient:

$$\lambda_d = 2gdS_w/v^2 \tag{1}$$

where λ_d is the resistance coefficient, d is flow depth, S_w is water-surface slope, and v is mean velocity (Davies, 1980). The various transverse rib configurations were quantified using effective roughness concentration, e (the sum of the heights of all roughness elements divided by the length of the sample) (Rouse, 1965) and by L/h (length from upstream end of one rib to downstream end of successive rib/rib height) (Davies, 1980).

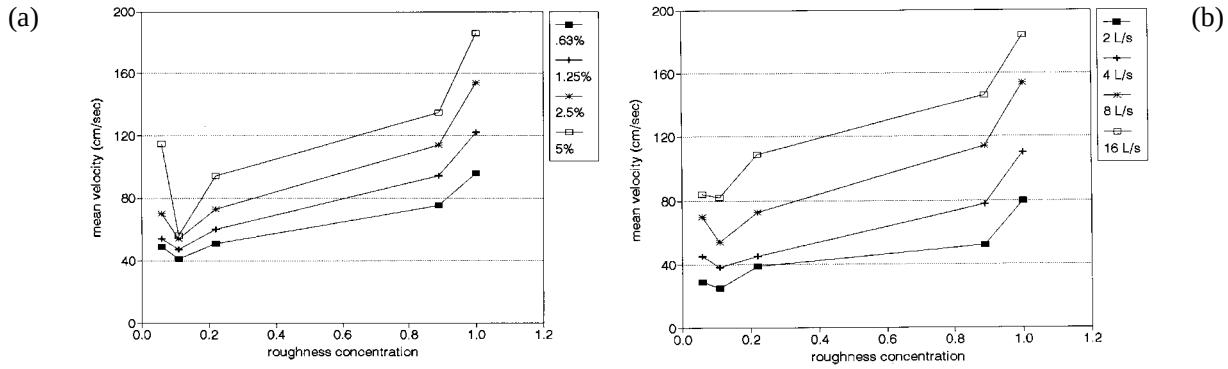

Figure 1. Roughness concentration versus mean velocity (a) for a discharge of 8 l s^{-1} and (b) for a slope of 2·5 per cent

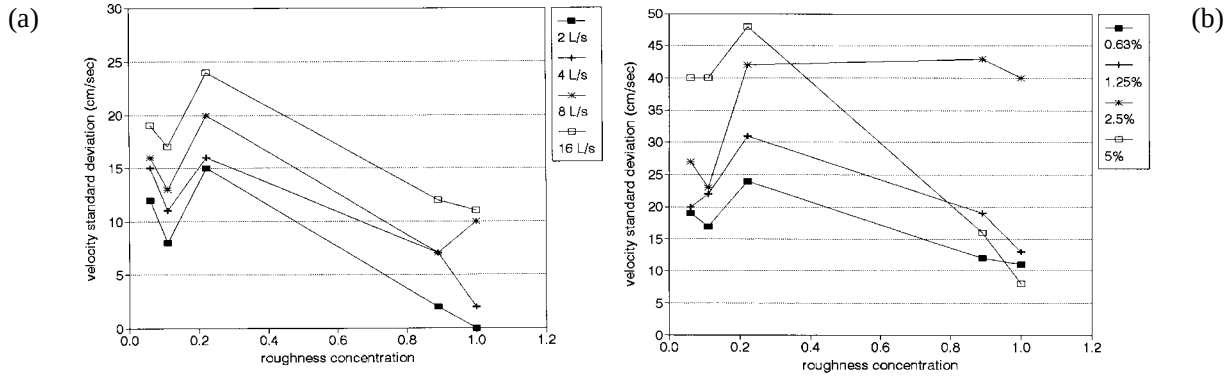

Figure 2. Roughness concentration versus velocity standard deviation (a) for a slope of 0·63 per cent and (b) for a discharge of 16 l s^{-1}

RESULTS

Transverse configurations and plane bed

Characteristics of reach-average mean velocity. For all cases, mean velocity consistently increased as channel slope and discharge increased. The rate of velocity increase was greatest at the highest values of slope and discharge (Table I). The range of mean velocity values among the 16 runs for each case decreased with e (i.e. the range was highest for Case 1). Mean velocity generally increased with increasing e, but with a sharp decrease at $e = 0{\cdot}06$–$0{\cdot}11$, and increases at $e = 0{\cdot}11$–$0{\cdot}22$ and $e = 0{\cdot}89$–$1{\cdot}00$ (Figure 1). Case 2 had the greatest difference in rate of velocity increase with discharge between high and low slopes, and Case 1 had the largest velocity increase with discharge. Reynolds numbers for the runs were in the range of 5000 to 10 000. Flow became supercritical downstream from the ribs for Case 4 at the larger values of discharge and slope.

Characteristics of reach-averaged velocity standard deviation. Standard deviation corresponded moderately well with channel slope and discharge for most cases, generally increasing with both slope and discharge in all cases but that of a plane bed, where standard deviation decreased with increasing slope. Statistical results were difficult to evaluate because of the very small datasets (degrees of freedom = 2), but values of R^2 were generally above 0·85. The trends of standard deviation in Cases 1–4 are probably influenced by the fact that for each run the flow measurements were located within different regions of the flow separation zone in the lee of the obstacle because, although the measurement points were fixed, the length of the flow separation zone changed as the spacing of obstacles changed. The trends of standard deviation in Cases 1–4 may also be related to the frequency of vortex shedding. The Strouhal number (nd/v, where n is frequency of vortex shedding, d is obstacle length, and v is mean velocity) remains approximately constant for Reynolds numbers in the range of 10^3–10^5. In these experiments, obstacle length remained constant, so as mean velocity increased, the frequency of vortex shedding should also have increased.

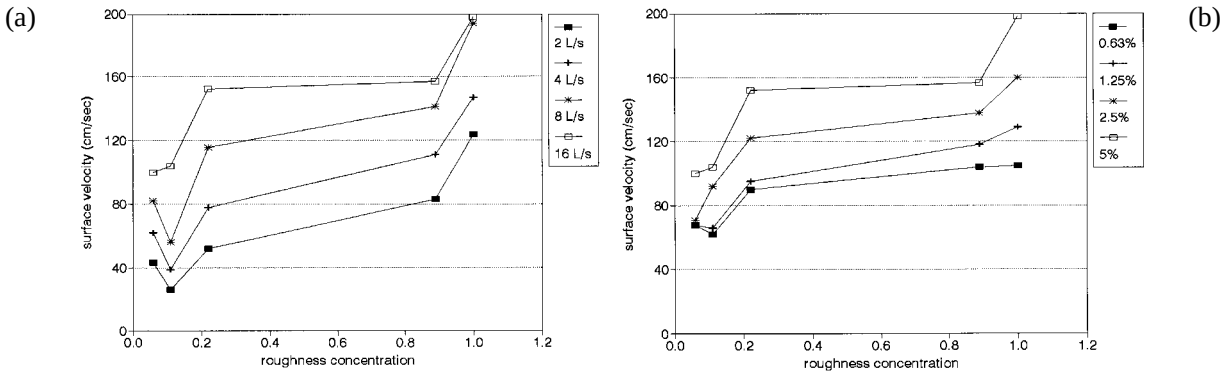

Figure 3. Roughness concentration versus surface velocity (a) for a slope of 5 per cent and (b) for a discharge of 16 l s^{-1}

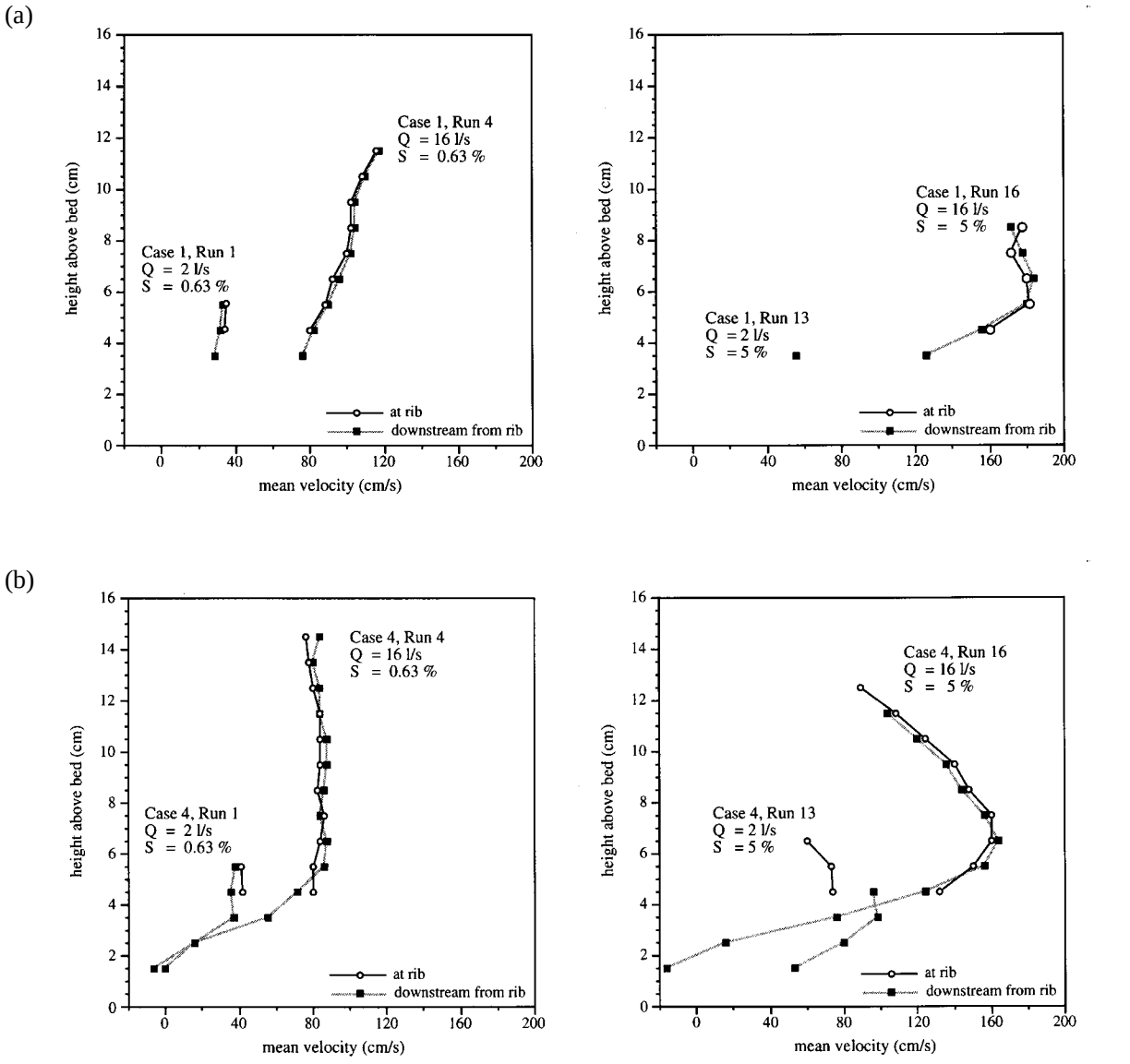

(c)

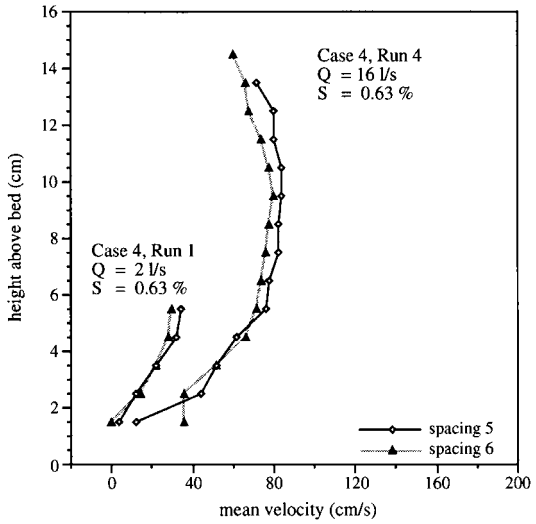

Figure 4. Vertical velocity profiles. (a) Case 1, for slopes of 0·63 and 5 per cent at 2 and 16 l s^{-1} at and immediately downstream from a rib. (b) Case 4, for slopes of 0·63 and 5 per cent at 2 and 16 l s^{-1} at and immediately downstream from a rib. (c) Case 4, for slopes of 0·63 and 5 per cent at 2 and 16 l s^{-1} at measurement points five and six rib-widths downstream from a rib

For a discharge of 16 l s^{-1}, standard deviation peaked dramatically at a 2·5 per cent slope when e was high (Case 1), but tended to peak at 5 per cent slope for low e values. The range of standard deviation values among the 16 runs decreased with e. For a given slope or discharge, the general trend of standard deviation was to decrease as e increased. Superimposed on this were steep decreases in standard deviation at e=0·06–9·11 and e=0·89–1·00, and an increase at e=0·11–0·22 (Figure 2).

Characteristics of reach-averaged surface velocity. Surface velocity corresponded well with channel slope and discharge, tending to increase as both slope and discharge increased. The increase of surface velocity with slope was most pronounced at the highest discharges and the highest e values. Similarly, the increase with discharge was most pronounced for the highest slopes. The range of surface velocity values for a given case decreased as e decreased. Surface velocity tended to increase as e increased, with a consistent sharp decrease at e=0·06–0·11, and increases at e=0·11–0·22 and e=0·89–1·00 (Figure 3).

Spatial patterns of velocity along the channel centreline. The vertical velocity profiles over and immediately downstream from the transverse ribs indicate that profile shape remains fairly constant for a given slope and roughness configuration as discharge increases (Figure 4). As slope increases, the profiles become less linear, with a much larger near-bed velocity gradient and a more pronounced velocity peak close to 0·6 flow depth (Figure 4). The near-bed velocity gradient immediately downstream from the rib is most pronounced at lower roughness concentrations (Cases 3 and 4). Velocity profiles several rib-widths downstream from a rib show similar tendencies, although the near-bed velocity gradient decreases markedly in a downstream direction (Figure 4c). Isovel maps of the channel centreline indicate similar trends, and show that the highest velocities, which tend to be over the rib at lower slopes, shift further downstream at higher slopes as the flow becomes supercritical between ribs, with the effect most pronounced at low roughness concentrations (Figure 5). In addition, the zone of large near-bed velocity gradients increases in both length and depth as roughness concentration decreases.

Resistance coefficient. The plot of resistance coefficient shows a clear maximum at L/h=8·95 for all values of slope and discharge (Figure 6). In general, for a given L/h configuration, the value of the resistance coefficient decreases as discharge increases and as slope decreases (Table I).

Longitudinal configurations

Characteristics of reach-averaged mean velocity. Mean velocity correlated well with both channel slope and discharge (values of R^2 consistently above 0·90), increasing with both slope and discharge for both channel-bed

(a)

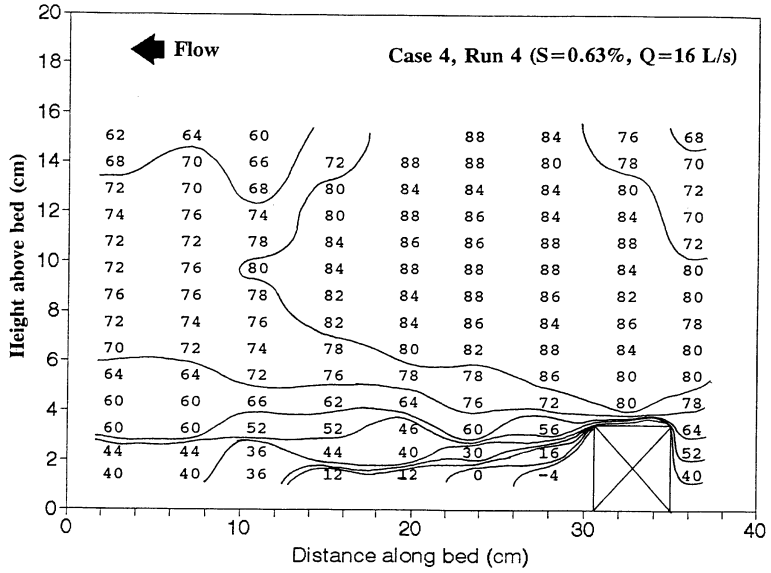

(b)

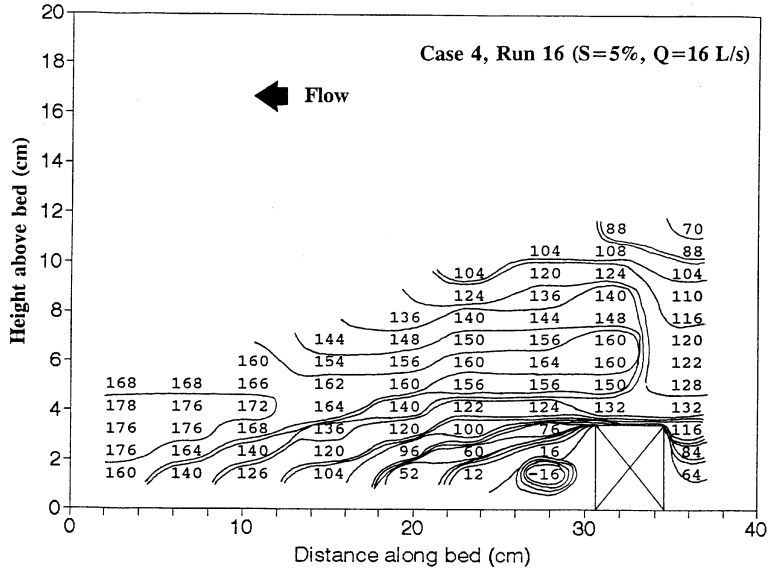

Figure 5. Isovelocity contours along the channel centreline downstream from a rib. Flow is from right to left, and contour intervals are 10 cm s^{-1}. Block with cross at lower right represents side view of rib. Water-surface elevation is non-uniform

configurations. The increases in velocity with increasing slope were most linear at lower discharges. For the lower values of slope and discharge, Case 6 always had higher velocities, but the velocity values for both cases tended to merge at a 5 per cent slope at discharges of 4 l s^{-1} and higher.

Characteristics of reach-averaged standard deviation. Standard deviation generally increased as discharge increased for both cases. Standard deviation increased markedly to slopes of 2·5 per cent in both cases and for all discharges, and then increased slightly or declined at 5 per cent slope. Case 6 had higher values of standard deviation at slopes of 2·5 and 5 per cent, and at higher discharges; Case 7 values were higher up to 1·25 per cent slopes for discharges of 2, 4 and 8 l s^{-1}

Characteristics of reach-averaged surface velocity. Surface velocity increased fairly regularly as both slope and discharge increased, with the steepest increases occurring up to 1·25 per cent slope and 4 ls^{-1}. Surface

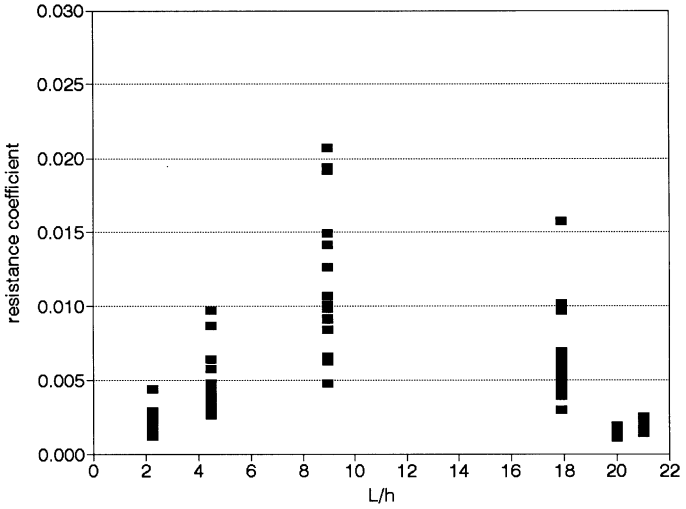

Figure 6. Resistance coefficient versus *L/h*. Each point represents an individual flume run (*L/h* values do not apply to longitudinal configurations, which are arbitrarily placed with respect to the *x*-axis at values of 20 and 21)

velocity is generally higher for Case 6 at lower slopes and discharges, and higher for Case 7 at higher slopes (2·5 and 5 per cent) and discharges (8 and 16 $l s^{-1}$).

Spatial patterns of velocity across the channel. Vertical velocity profiles, and velocity contours across the channel, indicate that steep velocity gradients develop above the space between ribs as discharge increases at low slopes, whereas steep near-bed velocity gradients develop within the inter-rib space with increasing discharge at high slopes. Velocities were generally larger, and velocity gradients more pronounced, for the more widely spaced ribs of Case 6.

DISCUSSION

For the transverse configurations, both surface and mean velocity increased as slope, discharge, relative roughness (*d/h*), and effective roughness concentration increased. For a given discharge, velocity increased as slope increased and relative roughness (*d/h*) decreased; the flume data do not permit us to isolate the relative importance of slope versus relative roughness. The rate of increase for mean and surface velocity was greatest at the highest values of slope and discharge; that is, for a given roughness value, velocity increase with discharge was always greatest at 5 per cent slope, and velocity increase with slope was greatest at 16 l s^{-1}. Among the four roughness configurations, Case 2 had the greatest difference in rate of velocity increase with discharge between high and low slopes, and Case 1 had the largest velocity increase with increasing discharge at all slopes (Table I). At low slopes, Case 2 had the lowest velocity increase with discharge, whereas at high slopes Case 4 had the lowest velocity increase with discharge. This suggests that the more widely spaced roughness elements of Cases 3 and 4 would be most effective at creating flow resistance over a range of discharges in channels with steeper slopes. The rectangular, sharp-edged ribs attached to a flat wooden bed in this experiment only crudely approximate natural bedforms such as ripples, dunes or bed-steps. However, we think it is reasonable to note some general parallels between flow resistance in natural channels and the flume results. At slopes of 2·5 per cent and 5 per cent, Cases 3 and 4 approximate the spacing of bed-steps in natural channels (Wohl and Grodek, 1995), and satisfy the criteria of Abrahams *et al*. (1995) for maximum flow resistance. Similarly, the more closely spaced roughness elements of Case 2 approximate the lower end of the current ripples, with length/height ratios begining at 5, that form in relatively low-gradient natural channels (Reineck and Singh, 1975).

Flow resistance may be evaluated using different approaches. Case 3 ($L/h = 8{\cdot}95$) has the maximum values of resistance coefficient at all discharges and slopes (Figure 6). These results confirm the findings of Johnson and

Le-Roux (1946) that maximum resistance occurs at *L/h* values of approximately 10 for short-crested roughness elements, and of Davies (1980) for ripples. Rouse (1965) defined *e* values of 0·15–0·25 as the maximum effective roughness concentration for producing flow resistance. Our results for all discharges and slope scenarios suggest that maximum resistance, as indicated by minimum mean velocity and maximum velocity standard deviation for a given slope and discharge, occurs at slightly lower roughness concentrations. Minimum mean velocity consistently occurred at $e = 0{\cdot}11$, or Case 3 (Figure 1), where ribs are seven rib-widths apart, whereas maximum standard deviation occurred either in Case 2 or Case 4 (Figure 2). Similarly, the near-bed velocity gradients are steepest over a large zone at the low roughness concentrations of Cases 3 and 4 (Figure 4). This suggests larger average lift forces, greater turbulence, and thus enhanced potential for sediment entrainment and transport at these configurations (Nelson *et al*., 1993, 1995).

For the longitudinal configurations, the two cases had very similar values of mean and surface velocity and standard deviation (Table I). In both cases, the highest velocities were along the channel bed between the grooves at high slopes, whereas at low slopes the highest velocities were well above the grooves. The longitudinal configurations always had higher values of mean and surface velocity, and lower values of the resistance coefficient, than the transverse roughness configurations. The transverse configurations generally had higher values of velocity standard deviation as well, suggesting that transverse roughness elements are more effective than longitudinal elements in creating resistance to flow and increased energy expenditure, presumably because form drag dominates over skin friction drag in these experiments. The results may partly explain the much greater frequency of occurrence of transverse roughness features in natural channels. Allen's (1969) experiments with erosional current marks indicated that longitudinal grooves form under lower current intensities, and are replaced by transverse erosional marks as current intensity increases.

CONCLUSIONS

Our results replicate earlier work in that they indicate a maximum value of resistance coefficient at a roughness *L/h* ratio of about 9 for all values of discharge and slope. In addition, the data suggest that discharge has little effect on velocity profile shape, whereas slope and roughness concentration substantially change profile shape, with maximum near-bed velocity gradients at steep slopes and relatively low roughness concentrations (*L/h* ratio of 9–18). Relative rates of mean velocity increase suggest that high roughness concentrations are more effective at creating flow resistance at lower slopes than at higher slopes. Longitudinal roughness configurations designed to mimic longitudinal grooves observed along natural channels caused much less flow resistance than did transverse configurations.

ACKNOWLEDGEMENTS

This work was performed while E.W. was on a fellowship from the Japan Society for the Promotion of Science. We thank Kenshiro Yamamoto, Akio Hara, Akio Nakano and Hideo Iijima for valuable assistance in running the flume experiments, Doug Thompson for helpful reviews, and Dan Cenderelli for assistance with drafting. Suggestions from two anonymous reviewers substantially improved the manuscript.

REFERENCES

Abrahams, A. D., Li, G. and Atkinson, J. F. 1995. 'Step–pool streams: Adjustment to maximum flow resistance', *Water Resources Research*, **31**, 2593–2602.

Allen, J. R. L. 1969. 'Erosional current marks of weakly cohesive mud beds', *Journal of Sedimentary Petrology*, **39**, 607–623.

Davies, T. R. H. 1980. 'Bedform spacing and flow resistance', *Journal of the American Society of Civil Engineers, Hydraulics Division*, **106**, 423–433.

Hassan, M. A. and Reid, I. 1990. 'The influence of microform bed roughness elements on flow and sediment transport in gravel bed rivers', *Earth Surface Processes and Landforms*, **15**, 739–750.

Johnson, J. W. and LeRoux, E. A. 1946. 'Flow in a channel of definite roughness', *Transactions, American Society of Civil Engineers*, **111**, 555–566.

Morris, H. M. 1995. 'Flow in rough conditions', *Transactions, American Society of Civil Engineers*, **120**, 373–398.

Nelson, J. M., McLean, S. R. and Wolfe, S. R. 1993. 'Mean flow and turbulence fields over two-dimensional bed forms', *Water Resources Research*, **29**, 3935–3953.

Nelson, J. M., Shreve, R. L., McLean, S. R. and Drake, T. G. 1995. 'Role of near-bed turbulence structure in bed load transport and bed form mechanics', *Water Resources Research*, **31**, 2071–2086.
Nowell, A. R. M. and Church, M. 1979. 'Turbulent flow in a depth-limited boundary layer', *Journal of Geophysical Research*, **84**, 4816–4824.
Reineck, H. -E. and Singh, I. B. 1975. *Depositional Sedimentary Environments*, Springer-Verlag, New York, 439 pp.
Robert, A., Roy, A. G. and De Serres, B. 1992. 'Changes in velocity profiles at roughness transitions in coarse grained channels', *Sedimentology*, **39**, 725–735.
Rouse, H. 1965. 'Critical analysis of open-channel resistance', *Journal of the American Society of Civil Engineers, Hydraulic Division*, **91**, 1–25.
Whittaker, J. G. and Jaeggi, M. N. R. 1982. 'Origin of step–pool systems in mountain streams', *Journal of the American Society of Civil Engineers, Hydraulics Division*, **108**, 758–773.

